

## An Electrochemical Quartz Crystal Microbalance (EQCM) Based on Microelectrode Arrays Allows to Distinguish between Adsorption and Electrodeposition

M. Biermann<sup>1</sup>, C. Leppin<sup>1\*</sup>, A. Langhoff, T. Ziemer<sup>2</sup>, C. Rembe<sup>2</sup>, D. Johannsmann<sup>1</sup>

1 Institute of Physical Chemistry, Clausthal University of Technology, Arnold-Sommerfeld-Str. 4, D-38678 Clausthal-Zellerfeld

2 Institute of Electrical Information Technology, Clausthal University of Technology, Leibnizstraße 28, D-38678 Clausthal-Zellerfeld

\*correspondence: christian.leppin@tu-clausthal.de

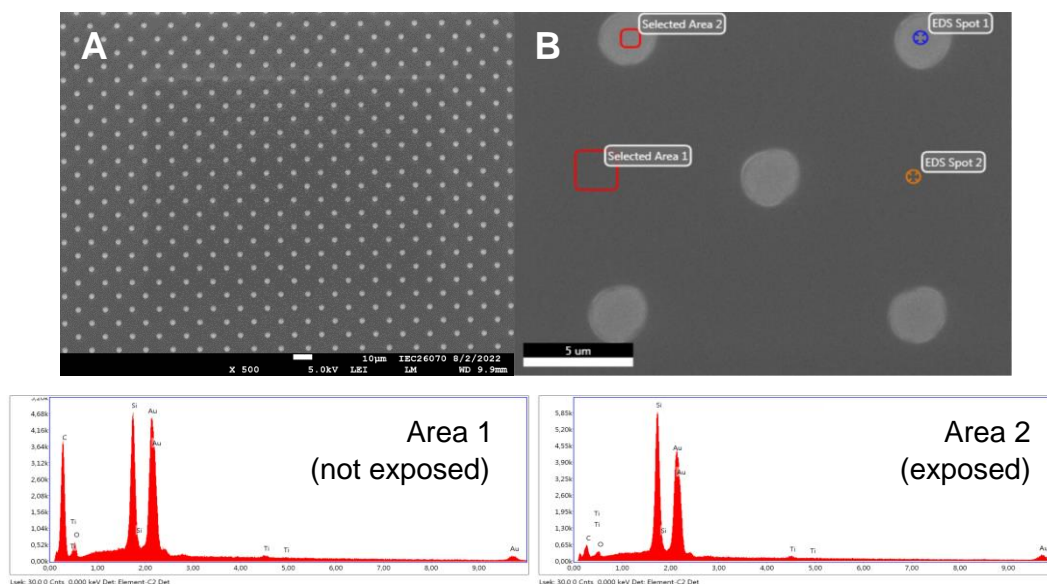
### Supporting Information

#### Characterization of the Microelectrode Arrays (MEAs)

For analyzing the preparation procedure and the MEA geometry, imaging, and spectroscopic studies on an exemplary MEA with a small diameter and a small pitch (dimensions:  $d = 2.5 \mu\text{m}$ ,  $p = 10 \mu\text{m}$ ) were carried out because this smaller microstructure is more vulnerable to preparation artifacts.

#### 1 Scanning Electron Microscopy

Imaging and energy dispersive X-ray spectroscopy (EDX) was performed on a JSM7610F Scanning Electron Microscope (JEOL, Akishima, Japan) at the Institute of Electrochemistry (TU Clausthal), using excitation energies of 5 keV and 15 keV, respectively. Before imaging, the surfaces were rinsed with ultra-pure water to remove residual electrolyte. The MEA shown in Fig. S 1 is regularly patterned and does not show any artifacts related to the electrode geometry. The pitch and the electrode diameter deviate from the targets by less than 10%. Despite the limited sensitivity of EDX to carbon due to the small photoelectric cross-section, it can be inferred that there is most likely no remaining photoresist in the areas forming the individual microelectrodes in Fig. S 1 B. The carbo peak is much decreased for the electrode areas/spots compared to the areas/spots covered with photoresist as shown in Fig. S 1 Area 1 and Spot 2.



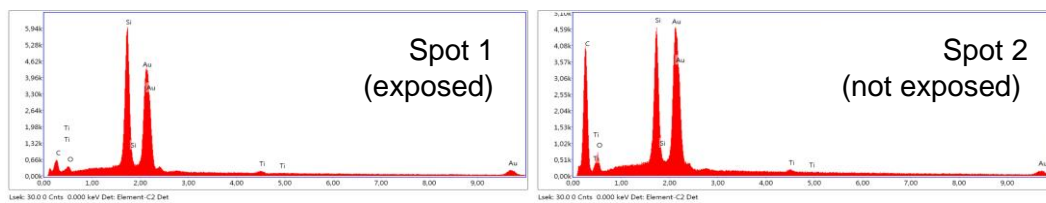


Fig. S 1: SEM image of an MEA (A) and close-up with highlighted spots of the EDX analysis. The EDX analysis yielded a lower carbon fraction in the light-exposed areas due to the absence of the polymer backbone.

## 2 Confocal Raman Microscopy

In order to verify that the photoresist was entirely removed from the electrodes, Raman spectra at different spots on the MEA were taken with an alpha300R Raman microscope from WITec (Oxford Instruments, Oxford, Great Britain). A 532 nm laser is used for excitation. From the Raman spectra obtained on areas covered and not covered with photoresist in Fig. S 2, it can be inferred that there is no remaining photoresist in the light-exposed areas. To perform Raman spectroscopy on the MEA, the laser power had to be decreased from 10 mW to 0.1 mW to avoid beam damage.

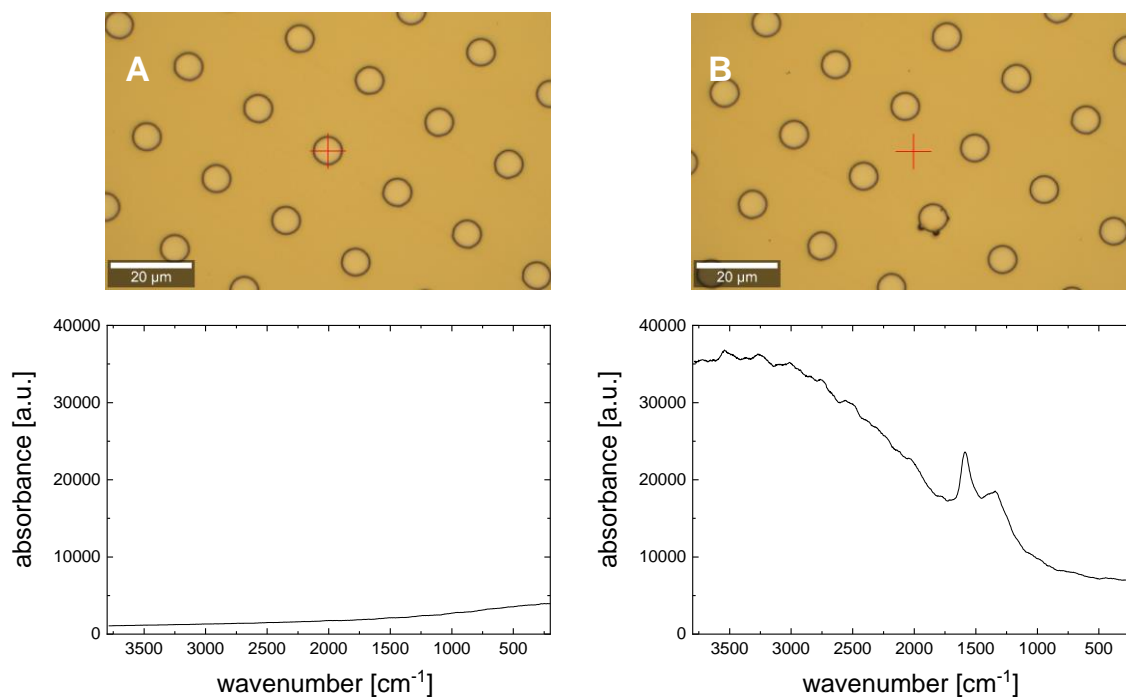


Fig. S 2: Raman spectra obtained in areas exposed (A) and not exposed (B) to the light. The absence of Raman bands on the exposed spots proves that there is no remaining photoresist on the microelectrode sites.

### 3 Atomic Force Microscopy

The height of the microstructures prepared on the resonators is not accessible to the SEM. In order to quantify the topography, AFM images were taken. Imaging was performed in tapping mode on a Park NX12 instrument (Park Systems, Suwon, Korea), employing AC160 TS cantilevers from Park Systems. The sharp edges of microelectrodes lead to so-called parachuting artifacts even with large P-gain. They are evident in Fig. S 3 as a shadow at the electrode edges along the scan-direction. Despite the high P-gain, the thickness of the blocking layer can still be determined to be  $\sim 1 \mu\text{m}$ .

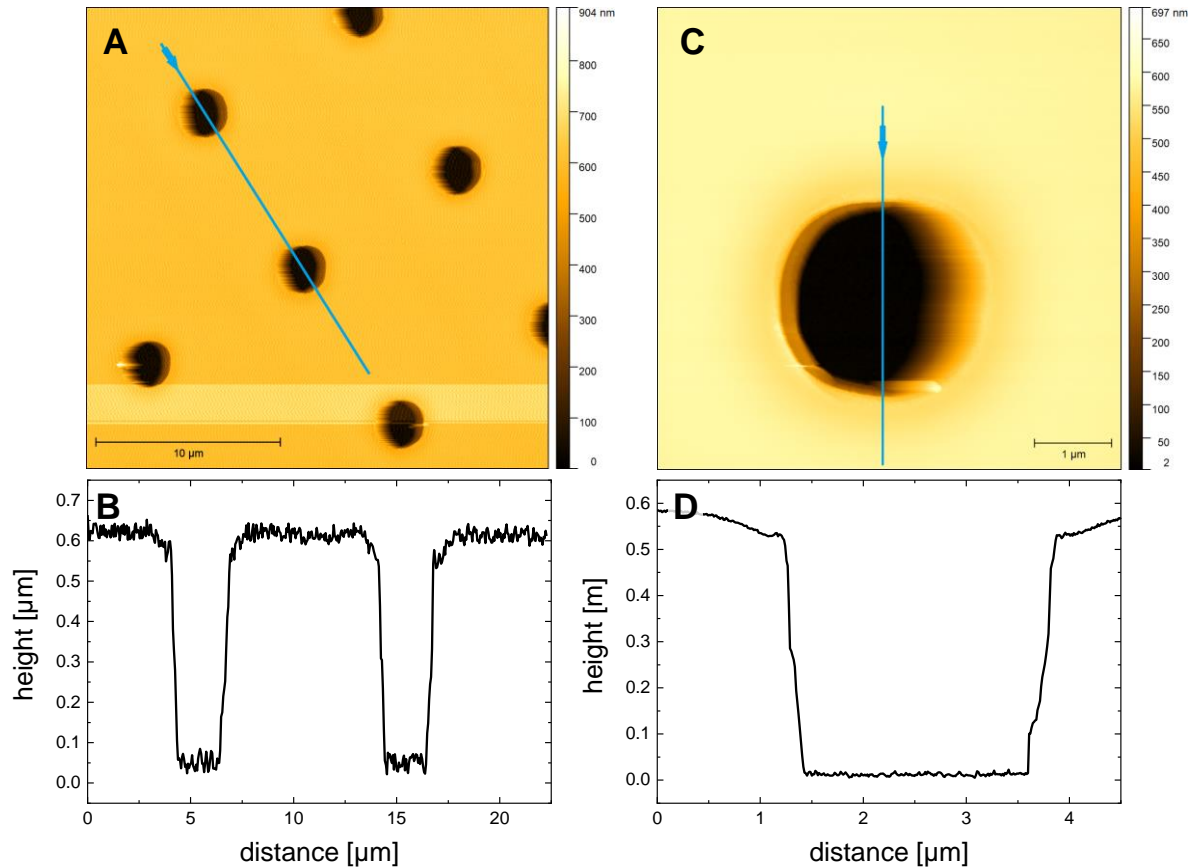


Fig. S 3: AFM image of an MEA showing a few microelectrodes (A) and a line profile (B). Close-up of one single microelectrode (C) and the corresponding line profile (D). In scan direction (A: left to right, C: right to left), parachuting artifacts are present due to the sharp edges of the microstructures.

#### 4 Confocal Laser Scanning Microscopy

Confocal Laser Scanning Microscopy (CLSM) also allows to study a sample's topography. The sample was scanned with a 408 nm laser in a VK-X210 CLSM (Keyence, Osaka, Japan). The micrograph in Fig. S 4A shows line-shaped artifacts in the photoresist related to the light exposure in the preparation procedure. However, the blocking layer does not suffer from these artifacts because they do not reach the electrode surface as depicted in the topography projection in Fig. S 4 B. Although CLSM suffers from the interference of light at the edges, the line profile in Fig. S 4 C can confirm the thickness of the insulating photoresist to be  $\sim 1 \mu\text{m}$ .

